

# Spectroscopic characterization of mucilage (Chia seed) and polygalacturonic acid

Ruth H. Ellerbrock<sup>1\*</sup>, Mutez Ali Ahmed<sup>2</sup>, and Horst H. Gerke<sup>1</sup>

<sup>1</sup> Leibniz Centre for Agricultural Landscape Research (ZALF), Research Area 1 "Landscape Functioning", Working Group "Hydropedology", Eberswalder Strasse 84, 15374 Müncheberg, Germany

<sup>2</sup> University Bayreuth, Chair of Soil Physics, 95447 Bayreuth, Germany

## Abstract

Polygalacturonic acid (PGA) has frequently been suggested and used as a model substance for studying mucilage properties and effects in soil. While PGA has a defined chemical structure, the composition of mucilage as natural product can vary in space and time depending on the plant and soil conditions. However, it is still unclear if PGA can be used as surrogate for original mucilage when considering soil–mucilage interactions in the rhizosphere. Here the organic matter (OM) composition of PGA was compared with that of Chia seed mucilage and small-scale spatial distribution of OM composition in mucilage droplets was analysed using Fourier transform mid infrared spectroscopy in KBr-transmission technique (FTIR). Selected regions of dried Chia seed mucilage droplets were analysed using micro-Fourier transform mid infrared spectroscopy in transfection technique (micro-FTIR).

For PGA, the FTIR spectra revealed lower C–H/C=O and higher C=O/C–O–C ratios as compared to Chia seed mucilage, indicating a relatively lower potential hydrophobicity and higher sorption capacity of the OM in PGA than OM in mucilage. The micro-FTIR spectra revealed that the potential hydrophobicity of a single freeze-dried mucilage droplet was higher at the tip as compared to regions located above the tip. The results suggest that the use of PGA as model substance for mucilage is limited especially when trying to imitate the sorption and wettability properties of the Chia seed mucilage OM. The spatial heterogeneity in OM composition as well as shifts in maxima of C=O and O–H bands in micro FTIR spectra of the cross sectioned mucilage droplet suggest that the composition of mucilage is changing with time. These findings may help initiating future studies on the dynamics and variability of OM composition of mucilage.

**Key words:** FTIR / KBr transmission technique / local-scale distribution / micro-FTIR spectroscopy

Accepted July 25, 2019

## 1 Introduction

Root exudates comprise mucilage (Angst et al., 2016; Kögel-Knabner, 2017) and other organic components like amino acids, vitamins, and polysaccharides. After exudation, mucilage is dynamically changing due to bio-chemical and physical processes when it comes in contact with soil minerals (McCully, 1999), especially cations (Marx et al., 2007), or because of the activity of micro-organisms (White et al., 2016). Due to aging processes (*i.e.*, drying, complexation, decomposition), mucilage composition varies in space and with time (Gregory et al., 2013), thereby again affecting physico-chemical properties (Kroener et al., 2014; Ruiz et al., 2015). Since composition and properties of mucilage are widely unknown and its collection is not easy, polygalacturonic acid (PGA) was often considered as a simplified model (Morel et al., 1987; Mimmo et al., 2003) and used to simulate the behavior of mucilage (*e.g.*, Czarnes et al., 2000; Gaume et al., 2000; Chen and Arye, 2017).

As for mucilage, also PGA contains a significant proportion of labile polysaccharides (Jones and Edwards, 1998) and shows

some similar characteristics (Morel et al., 1987; Gessa and Deiana, 1992; Mikutta et al., 2006). However, PGA is a defined chemical component, while mucilage represents a mixture of proteins and polysaccharides, among others, that may dynamically change (Carminati and Vetterlein, 2013; Naveed et al., 2019). Amount and composition of mucilage are affected by plant type, age, and soil conditions (Jones et al., 2009; Carvalhais et al., 2011; Ahmed et al., 2015, 2018a), and may vary in its composition in a wider range than PGA. The mucilage and derivatives resulting from such aging processes (Nguyen et al., 2008) contribute (together with the OM of decaying roots) to the formation of organo-mineral coatings along the root channels and the stabilization of aggregates (*e.g.*, Ahmed et al., 2018b; Di Marsico et al., 2018;). Changes in the OM composition of root cell walls caused by decomposition were recently described (White et al., 2016). Still, questions on the (1) temporal variability in composition of mucilage that potentially results in heterogeneity of the spatial distribution of mucilage composition and (2) applicability of PGA for simulating the behavior and properties of mucilage remain open.



\* Correspondence: R. H. Ellerbrock; e-mail: rellerbrock@zalf.de

The OM composition is related to properties such as wettability (Capriel, 1997; Chenu et al., 2000; Haas et al., 2018) or cation exchange capacity (Celi et al., 1997; Kaiser et al., 2008). The term composition describes amount and content of functional groups like hydroxyl- (OH), alkyl- (C–H), carbonyl- and carboxyl-groups (summarized here by C=O) within OM. Spectroscopic techniques like nuclear magnetic resonance (NMR) or Fourier Transform infrared spectroscopy (e.g., Kögel-Knabner, 1997; Gerzabek et al., 2006; Demyan et al., 2012) allow determining type and content of such functional groups. The properties of OM at surfaces of macropores including decayed root channels (Ellerbrock and Gerke, 2004; Leue et al., 2013) can play an important role during preferential flow and transport of reactive solutes by controlling mass transfer between flow paths and the soil matrix (e.g., Gerke, 2006; Cheng et al., 2017; Leue et al., 2013, 2018). However, the contribution of mucilage to OM composition of root channel surfaces is widely unknown.

The objective of our study was to evaluate the applicability of using PGA as a surrogate for original plant mucilage and to test if the OM composition of mucilage is uniformly distributed within exuded mucilage. Fourier Transform mid-infrared spectroscopy in KBr-transmission technique (FTIR) was used to compare the OM composition of PGA and mixed Chia seed mucilage and mm-scale variability in a mucilage droplet, and micro-FTIR spectroscopy was used to account for micro-scale spatial variability of OM composition.

## 2 Material and methods

The mucilage was collected from Chia seeds as described by Ahmed et al. (2014, 2015). Briefly, Chia seeds were mixed with water at a gravimetric ratio of 1 to 10. The mixture was stirred for 2 h and then it was passed through two sieves. The mucilage formed a larger droplet that was immediately freeze-dried such that the shape was conserved (Fig. 1). Analyses were carried out with mid infrared light by using (1) Fourier transform infrared spectroscopy in KBr-transmission technique (FTIR) and (2) micro-Fourier transform infrared spectroscopy in transfection technique (micro-FTIR). The chemical composition of Chia seed mucilage is similar to that of maize mucilage: both are mainly composed of xylose, glucose, and uronic acids. In both, maize and Chia seed mucilage, the content of uronic acid is about 25% (Lin et al., 1994; Carminati and Vetterlein, 2013). Mucilage from Chia seeds has a similar physical behavior to that of mucilage from maize and lupine and contains significant amounts of polysaccharides that form a gel-like network around the seeds (Lin et al., 1994; Muñoz et al., 2012).

For FTIR (Ellerbrock et al., 1999) half of the freeze-dried mucilage droplets were homogenized using an impact mill to obtain mixed mucilage samples. We noticed that homogenization could not fully be achieved. Some brownish-colored particles remained after the homogenization procedure in the mucilage samples that could be observed by naked eye. Alternatively, a freeze-dried mucilage droplet (Fig. 1) was studied by spatially-localized sampling of the droplet tip (M12<sub>0-5</sub>) and regions 20 mm above the tip, the latter regions

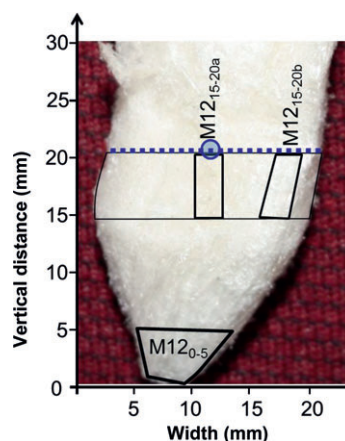


**Figure 1:** Photo of the vertical cross-section of a freeze-dried mucilage droplet on reddish patterned background and sampling scheme indicating the regions of extraction of M12<sub>0-5</sub>, M12<sub>5-20a</sub>, and M12<sub>15-20b</sub> samples (black lines); the vertical distance is measured from the tip of the mucilage droplet upwards. The blue dotted line indicates the position from which a layer of about 2 mm thickness was obtained for carrying out the micro-FTIR measurements along a transect of 0.13 mm length.

were separated into an outer (M12<sub>15-20a</sub>) and a more central sample (M12<sub>15-20b</sub>).

An amount of 0.5 mg of these mucilage samples was mixed with 100 mg of KBr (spectroscopy grade; Merck), stored overnight in an exsiccator over silica-gel, then finely-ground in an agate mortar and pressed into pellets (Ellerbrock et al., 1999) for Fourier transform mid infrared (FTIR) analysis with a FTS135 (BioRad Corp, Hercules, CA, USA) using the KBr-transmission technique (Fig. 2a). The mixed mucilage sample was analysed in 11 replicates (M1–M11). The FTIR spectra of PGA (pale beige solid; Chemical Abstracts Service No.: 25990-10-7; CARL ROTH, Karlsruhe, Germany) were obtained by using 0.5 mg of PGA mixed with 100 mg of KBr as described above (also in 11 replicates). Each FTIR spectrum was recorded by 16 co-added scans at a resolution of 1 cm<sup>-1</sup> in the region of wave number (WN) 400 to 4000 cm<sup>-1</sup>. The empty sample chamber of the FTS135 was used to obtain the background spectra (Gottwald and Wachter, 1997).

For micro-FTIR, a 2 mm thick layer from another intact freeze-dried mucilage droplet was cut about 20 mm above the droplet tip (Fig. 1, blue dotted line) with a scalpel, fixed on an aluminum plate, and stored in a desiccator over silica gel for 16 h. Then, a 200 μm long micro-transect across the mucilage layer was analysed in ten steps of 20 μm distance from the center of the droplet towards the side (Fig. 1, blue circle). Micro-FTIR spectroscopy was carried out with a Cary 660 combined with a Cary 610 microscope (both from Agilent Technologies, Santa Clara, CA, USA). Each micro-FTIR spectrum was recorded by 4 co-added scans (i.e., 4 replicate spectra) at a resolution of 4 cm<sup>-1</sup> in the region of 680 to 4000 cm<sup>-1</sup> in transfection technique. During transfection (cf Bassan et al., 2009), the infrared light is (1) transmitted through the samples until (2) it is reflected at the aluminium plate, and (3) transmitted through the sample towards the

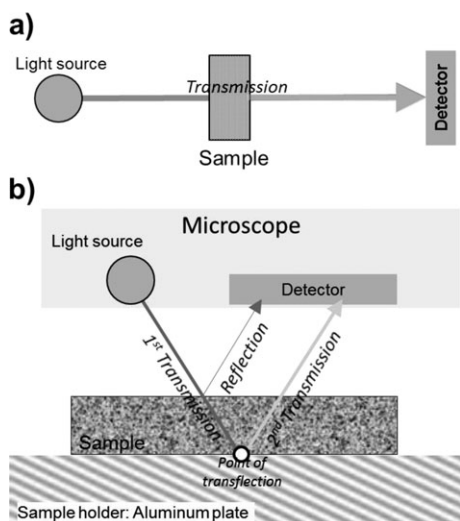


**Figure 2:** Schemes indicating differences in the IR light beam as used in (a) Transmission FTIR in KBr technique (a single light transmission) and in (b) micro FTIR technique where light is transmitted through the sample (1<sup>st</sup> transmission), reflected at the transfection point and re-transmitted (2<sup>nd</sup> transmission) towards the detector (cf Bassan et al., 2009).

detector (Fig. 2b). The micro-FTIR spectra are obtained in the unit  $\log(1/R)$ , where  $R$  is a measure for transmittance, and processed using the software WIN-IR Pro 3.4 (Digilab, MA, USA). Note that here the transmittance,  $R$ , is used in contrast to the reflectance which is known from the diffuse reflectance infrared Fourier transform (DRIFT) technique (Gottwald and Wachter, 1997). A gold target (99% Infragold<sup>®</sup>, Labsphere, North Sutton, NH, USA) fixed onto the positioning table was used as a background (cf Haas et al., 2018).

All spectra (FTIR and micro-FTIR) were corrected against ambient air as background (Haberhauer and Gerzabek, 1999) and smoothed using a “boxcar”-function ( $f = 105$  for KBr-transmission technique and  $f = 25$  for micro-FTIR; Win-IREZ software, BioRad). The spectra were baseline-corrected and normalized for the band at  $\text{WN } 1100 \text{ cm}^{-1}$  (e.g., Ellerbrock et al., 1999) and analysed according to Ellerbrock et al. (2009): the C–H band intensities were measured as a vertical distance (i.e., as height) from a local baseline plotted between tangential points in the spectral regions between  $\text{WN } 3100\text{--}2800 \text{ cm}^{-1}$ . The C=O band intensities were measured as heights from the global baseline of the spectra to the maxima within the regions of  $\text{WN } 1780$  to  $1710 \text{ cm}^{-1}$  and that at  $\text{WN } 1680$  to  $1580 \text{ cm}^{-1}$ . The stretching vibrations of C–O–C groups at  $1081 \text{ cm}^{-1}$  were denoted as C–O–C band. The intensity of the C–O–C band was measured as a vertical distance from the maximum of the C–O–C band to the global baseline (Kaiser et al., 2008). The C–H, C=O, and C–O–C absorption bands are interpreted to characterize OM composition with respect to functional OM properties because these bands can be distinguished from those of the soil minerals. These bands are used for estimating potential hydrophobicity in terms of the C–H/C=O ratio (Capriel, 1997; Ellerbrock et al., 2005) and potential sorption capacity in terms of the C=O/C–O–C ratio (Celi et al., 1997; Kaiser et al., 2008). Additionally, the O–H and C=O absorption

bands in FTIR spectra were used for analysing shifts in band maxima.

Mean values and standard deviations of C–H/C=O and C=O/C–O–C ratios obtained from FTIR spectra are calculated from 11 replicates after testing for outliers using the Nalimov test (Kaiser and Gottschalk, 1972; with  $r(p) = 1.916$  for  $p = 95\%$  and  $r(p) = 2.368$  for  $p = 99.9\%$ ). The significance of differences between the mean values of PGA versus mucilage for the C–H/C=O and C=O/C–O–C ratios was tested using a Student’s t-test (Kaiser and Gottschalk, 1972; with  $t(p) = 2.08$  for  $p = 95\%$  and  $t(p) = 3.85$  for  $p = 99.9\%$ ).

### 3 Results

The spectra of all samples (Figs. 3 and 4) show absorptions bands in the region of the hydroxyl (O–H bonds), alkyl (C–H), carboxyl and carbonyl (C=O), and polysaccharide (C–O–C) functional groups (Tab. 1). For PGA, the maximum of the O–H band in the FTIR spectrum (Fig. 3a) was found at  $\text{WN } 3439 \text{ cm}^{-1}$  (Tab. 1). In FTIR of mucilage samples (M1 to M11), the mean O–H band maximum is located at  $\text{WN } 3404 \text{ cm}^{-1}$  (Tab. 1). The FTIR spectra of PGA samples show also absorption bands in the region between  $\text{WN } 2600$  to  $2200 \text{ cm}^{-1}$  (grey circle in Fig. 3a) which are not present in the mucilage FTIR spectra. Absorption bands in this region indicate the presence of (1) N–H bonds in protonated primary and secondary amines or (2) O–H bonds in phosphoric acid derivatives (Gottwald and Wachter, 1997) possibly formed during PGA extraction procedure. Since PGA contains beside the COOH group a large amount of directly neighbored OH groups per monomer-unit hydrogen bridges between these groups may easily be formed which may also explain the absorption bands in the  $\text{WN } 2600$  to  $2200 \text{ cm}^{-1}$ .

The FTIR spectra of mucilage samples M12<sub>15–20a</sub> (droplet center) show a broad O–H band with the maximum at  $\text{WN } 3399 \text{ cm}^{-1}$ , while the O–H band maximum was at  $\text{WN } 3426 \text{ cm}^{-1}$  (Tab. 1) for samples M12<sub>0–5</sub> (droplet tip) and M12<sub>15–20b</sub> (droplet rim).

In the FTIR spectra of PGA samples, the maximum of the first C–H band (band a2; Fig. 3a) is located around  $\text{WN } 2929 \text{ cm}^{-1}$ , while for the mucilage samples, the maxima of these first C–H-bands are located near  $\text{WN } 2922 \text{ cm}^{-1}$  (band b2; Fig. 3b). While PGA shows two maxima for C=O at  $\text{WN } 1738 \text{ cm}^{-1}$  and  $1642 \text{ cm}^{-1}$  and for C–O–C bands at  $\text{WN } 1083$  and  $1021 \text{ cm}^{-1}$ , the mucilage samples have a single C=O band maximum at  $\text{WN } 1615 \text{ cm}^{-1}$ , a shoulder at  $\text{WN } 1711 \text{ cm}^{-1}$ , and a single C–O–C band located at  $\text{WN } 1052 \text{ cm}^{-1}$  (Tab. 1, Fig. 3b, c).

The FTIR spectra of the disturbed mucilage samples (M1–M11) show some variation in the absorption intensity of C–H and C=O bands (Fig. 3b). The t-tests indicate that the mean C–H/C=O ratio of about 0.262 is significantly higher for mucilage (99.9% level) than that of PGA samples (0.181; Tab. 2). The C–H/C=O and the C=O/C–O–C ratios of the mixed mucilage samples are in a similar range as compared to those of the M12<sub>0–5</sub>, M12<sub>15–20a</sub>, and M12<sub>15–20b</sub> samples (Tab. 3). For the C–H/C=O ratio, the mucilage values are all

**Table 1:** Number of absorption bands in the FTIR spectra, kind of functional group (O–H, C–H, C=O, C–O–C), range (wavenumber) of the OH, CH, C=O and C–O–C absorption bands, and location (wavenumber) of their maxima in FTIR spectra of (a) polygalacturonic acid (PGA), (b) mixed mucilage (M), and (c) mixed mucilage from 3 sample locations; standard deviations in brackets.

Bands <sup>#</sup>	O–H stretch	C–H stretch symmetric	C–H stretch asymmetric	C=O stretch	C=O, C=C stretch	C–O–C	C–O–C
Nr in Fig. 3	1	2	3	4	5	6	7
Range (cm <sup>-1</sup> )	3700–2700	2950–2800	2800–2700	1740–1698	1680–1580	1150–900	
Sample	Maxima at WN in cm <sup>-1</sup>						
(a) PGA; n = 11	3439 (6)	2929 (2)	2880 (4)	1738 (9)	1642□ (1)	1083* (7)	1021* (1)
(b) M; n = 11	3404 (7)	2922 (< 1)	2878 (2)	1711□ (< 1)	1615 (5)	1052 (< 1)	–
(c) M12_0–5	3426	2926	2859	1710□	1628	1055	–
M12_15–20a	3399	2924	2859	1710□	1618	1053	–
M12_15–20b	3426	2926	2859	1710□	1625	1054	–
Micro-transect	3414 (21)	2927 (3)	2859 (< 1)	1710□ (< 1)	1629 (5)	1104 (5)	

□: shoulder of an absorption band;  
 \*: double band.

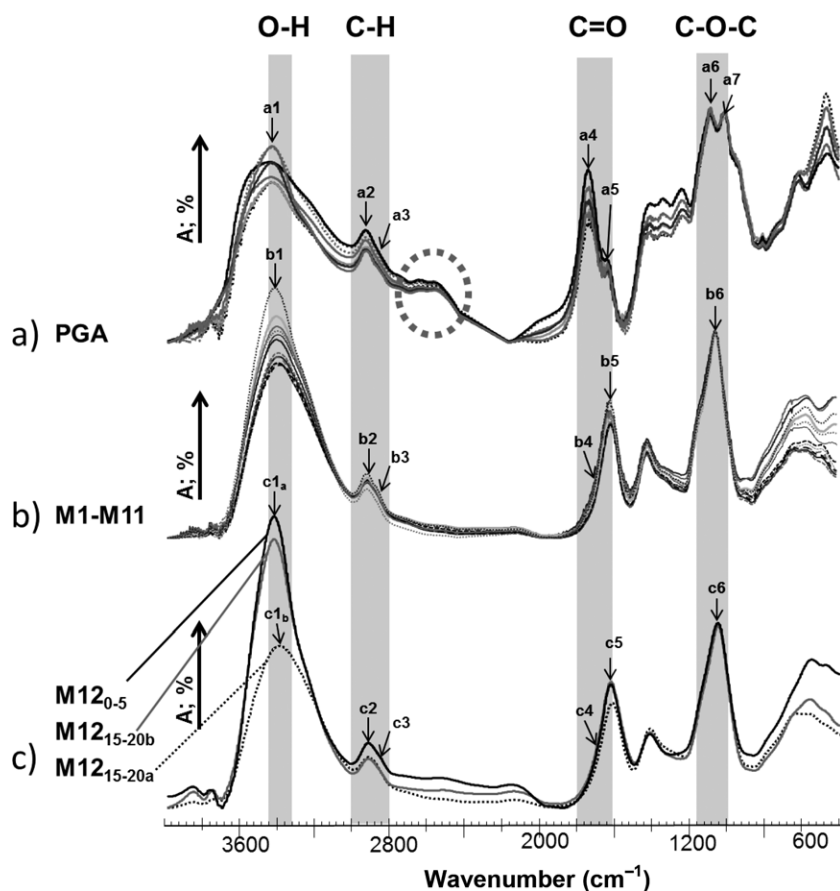


**Figure 3:** Mid-infrared spectra recorded by the transmission method and shown as absorption spectra ( $A = 100 - T$ ) of (a) six replicates of PGA, (b) 11 replicates of homogenized mucilage (M1–M11) from Chia seed, and (c) samples from selected regions (M12<sub>0-5</sub>; M12<sub>15-20a</sub>; M12<sub>15-20b</sub>) of a freeze-dried mucilage droplet. The letters indicate the maxima of O–H, C–H, C=O, and C–O–C absorption bands (cf Tab. 1): a1: 3439, a2: 2929, a3: 2879, a4: 1738, a5: 1642, a6: 1083, a7: 1021 cm<sup>-1</sup>; b1: 3404, b2: 2922, b3: 2878, b4: 1712, b5: 1615, b6: 1052 cm<sup>-1</sup>; c1<sub>a</sub>: 3426, c1<sub>b</sub>: 3399, c2: 2926, c3: 2859, c4: 1710, c5: 1628; c6: 1054 cm<sup>-1</sup>.

significantly larger than those of PGA (Tab. 2) while for the C=O/C–O–C ratio, the value of mixed mucilage is smaller (95% level) than that of PGA (0.942).

The micro-FTIR spectra (Fig. 4a) along a micro-transect located in the central part of a freeze-dried mucilage droplet indicate differences in the spatial distribution of the OM composition related to the position of the measurement points (Fig. 4b). Up to about 70 μm distance from the center the C=O/C–O–C ratios increase (Fig. 5) and then decrease. The smallest value of the C=O/C–O–C ratio (0.837; Fig. 5) at the beginning of the micro transect is larger than that of the (mixed) M12<sub>15-20a</sub> sample (Tab. 3) from the same location of another droplet.

The C–H/C=O ratios remain relatively constant at a level between 0.15 to 0.20 up to a distance of 82 μm and decrease only at greater distance (Fig. 5).

The WN's of the O–H band maxima for micro FTIR spectra of mucilage samples along the transect show an average shift (decrease) in WN of 35 cm<sup>-1</sup> as compared to the maxima observed for PGA (Tab. 1). The maxima of the O–H band in FTIR spectra of M12 samples seem to depend on the location within the mucilage droplet: Samples from the tip (M12<sub>0-5</sub>) and the rim (M12<sub>15-20b</sub>; Fig. 1) show a maximum at WN 3426 cm<sup>-1</sup> (Tab. 3) while sample from the droplet center (M12<sub>15-20a</sub>) have a maximum at lower WN of 3399 cm<sup>-1</sup> (Tab. 1). For the

**Table 2:** Mean values, standard deviation (SD) as well as minimum and maximum values (Min/Max) of the C–H/C=O and C=O/C–O–C ratios in FTIR spectra of mixed mucilage (M) and polygalacturonic acid samples (PGA).

Sample	C–H/C=O			C=O/C–O–C		
	Mean values	SD	Min/Max	Mean values	SD	Min/Max
PGA ( $n = 11$ )	0.181	0.0122	0.153/0.198	0.942	0.0850	0.811/1.097
M ( $n = 11$ )	0.262	0.0108	0.244/0.280	0.748	0.0616	0.685/0.847

**Table 3:** The wavenumber (WN) of OH and C=O band maxima and the C–H/C=O and C=O/C–O–C ratios in FTIR spectra (KBr technique) of selected mucilage samples.

Sample	WN ( $\text{cm}^{-1}$ )		Ratio	
	O–H band	C=O band	C–H/C=O	C=O/C–O–C
M12_0–5	3426	1628	0.221	0.984
M12_15–20a	3399	1618	0.209	0.799
M12_15–20b	3426	1625	0.161	1.055

cr-

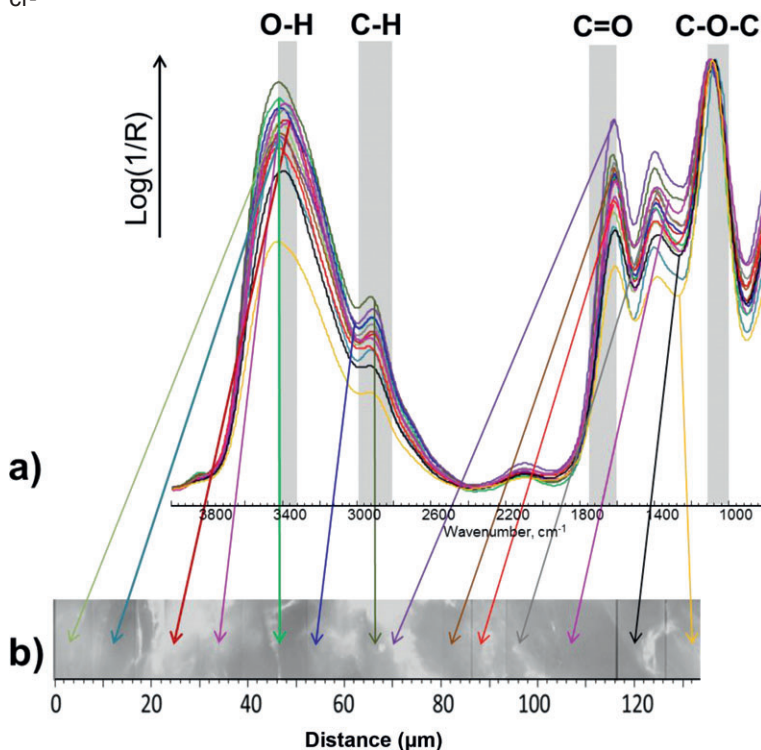


**Figure 4:** (a) Micro-FTIR spectra obtained from measurement points along an intact surface of a cross-sectioned mucilage droplet (cf Fig. 1) and (b) the black-and-white photo of the mucilage surface along the transect indicating locations of the measurement points.

cross-sectioned droplet (Fig. 4b), the maxima of the O–H bands in the micro FTIR spectra varied between WN  $3448 \text{ cm}^{-1}$  and WN  $3361 \text{ cm}^{-1}$  (Fig. 5). The variability of WN maxima for O–H band is larger than that of the WN maxima for C=O band, with largest variation of about  $19 \text{ cm}^{-1}$  (Fig. 5).

## 4 Discussion

### 4.1 Mucilage compared to PGA

The OM composition of mucilage and PGA can be compared by analysing differences in the WN values of the absorption band maxima (Tab. 1) and the relative heights of C–H and C=O absorption bands at the WN maxima. For PGA (Fig. 3a), a lower C–H/C=O ratio but a higher C=O/C–O–C ratio as compared to mucilage (Tab. 2) indicates a relatively lower potential hydrophobicity (C–H/C=O) but a higher sorption (e.g., cation exchange) capacity (C=O/C–O–C). Since the C–H/C=O ratios of PGA differ significantly (99.9% level) from those of Chia seed mucilage, the assumption that PGA could be used as an analogue

for Chia seed mucilage (e.g., Morel et al., 1987; Gessa and Deiana, 1992; Czarnes et al., 2000) seems to be questionable with respect to the tested OM properties (Ellerbrock and Gerke, 2013; Leue et al., 2013). These results are in agreement with recent observations of Zickenrott et al. (2016) who concluded that the Ca-salt of PGA is an inappropriate analogue when trying to mimic the behavior of root mucilage with respect to hydrophobicity.

### 4.2 Spatial heterogeneity of mucilage composition

The C–H/C=O ratios have been described as a measure for the potential wettability (Ellerbrock et al., 2005); here the values of the homogenized mucilage samples are in a similar range as those of the M12 samples selected from the freeze-dried droplet, except for M12<sub>15–20b</sub> (Tab. 3). The differences in the C–H/C=O ratios and the higher C=O/C–O–C ratio of M12<sub>15–20b</sub> as compared to M12<sub>15–20a</sub> and M12<sub>0–5</sub> indicate that OM composition is heterogeneously distributed within the droplet at milli- and at micro-meter scale. Thus, homogenized mucilage samples may not reflect the properties of Chia seed mucilage in natural conditions. The observed spatial heterogeneity in OM composition (in terms of relative C–H group content) corresponds with that observed by micro-FTIR across root channels of maize seedlings (Holz et al., 2018). As assumed by Carvalhais et al. (2011) and Ahmed et al. (2015), mucilage composition may be affected by growing conditions of the plants such that the composition of the excreted mucilage may vary with time causing heterogeneity in OM composition in space.

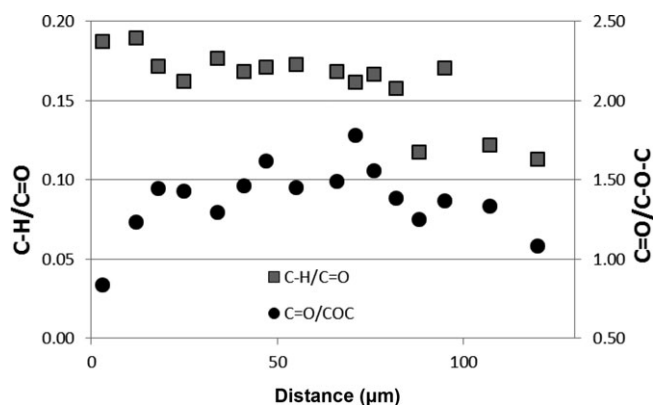


**Figure 5:** Evaluated C–H/C=O and C=O/C–O–C ratios from micro-FTIR spectra (Fig. 4a) plotted as a function of the distance along the micro-transect in Fig. 4b.

The OM composition of mucilage and its spatial heterogeneity may be of importance for describing flow and transport processes (Naveed et al., 2019) since mucilage provides OM components for coatings of pores formed by plant roots (e.g., Angst et al., 2016; Kögel-Knabner, 2017). Decayed root channels could serve as preferential flow paths (e.g., Jarvis, 2007) and the distributed OM properties of pore walls could affect the transport of reactive solutes. The OM components from mucilage contribute to physico-chemical properties of such flow path surfaces (e.g., Leue et al., 2013, 2018), which are important for describing transport processes in structured soils (e.g., Cheng et al., 2017) and parameterization of two-domain models (e.g., Gerke, 2006).

The spatial heterogeneity of OM composition across the mucilage droplet and the shifts in WN of band maxima (Figs. 5 and 6) are possibly caused by oxidation processes during mucilage droplet “harvesting” (Ahmed et al., 2014). More intensively oxidized mucilage OM at the droplet’s outer regions are likely to result in increased C=O/C–O–C and reduced C–H/C=O ratios towards the droplet rim as it was found for M12 samples (Tab. 3).

### 4.3 Shift in absorption band maxima

The shifts in the FTIR adsorption maxima for the O–H bands across the micro transect of the intact mucilage droplet relative to band maxima of PGA was found larger as compared to that of the C=O bands (Fig. 6). For the O–H band maxima, a shift may be explained by small differences in the water content that allow O–H groups to form either intra- and inter-molecular hydrogen bridges with and between other O–H and C=O groups (Gottwald and Wachter, 1997). Interactions of OM with water and cations affect the strength of the O–H bond such that O–H groups involved in inter-molecular hydrogen bridges can be identified by absorption bands in the region of WN 3600 to 3200  $\text{cm}^{-1}$ , while O–H groups involved in intra-molecular hydrogen bridges by absorption bands in the region of WN 3180 to 2700  $\text{cm}^{-1}$  (Gottwald and Wachter, 1997). For most locations at the micro-transect (Fig. 4), the maximum of the O–H bands was shifted towards lower WN values (Fig. 6) indicating an increased formation of intra-molecular hydrogen bridges. Note that the band of N–H bonds

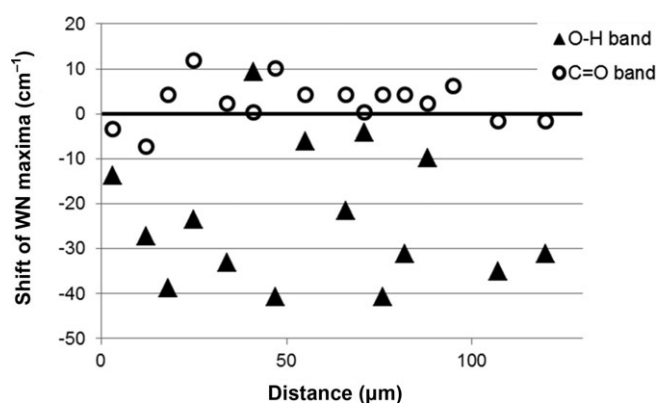


**Figure 6:** The shift of the wave numbers (WN) in  $\text{cm}^{-1}$  at absorption maxima of the C=O and the O–H bands in micro FTIR spectra of mucilage as compared to the mean maxima in FTIR of PGA (see Tab. 1) along the measurement transect (Fig. 4b).

within amines and amides (WN 3500 to 3300  $\text{cm}^{-1}$ ) cannot be identified here because these bands cannot be distinguished from the more intense O–H bands (Gottwald and Wachter, 1997).

Hydrogen bridges may also cause micelle-like structures within the gel-like structure of mucilage, e.g., forced by drying (e.g., Clapp et al., 1993). The observed shift in O–H band maxima (Fig. 6) may explain changes in the potential water storage capacity of mucilage (Ahmed et al., 2015; Carminati et al., 2017; Naveed et al., 2019). The shift could also result from interactions between O–H groups in mucilage and cations such as  $\text{Ca}^{2+}$  or  $\text{Al}^{3+}$  (Mimmo et al., 2003). More detailed studies on interactions and shifts in the WN maxima are beyond the scope here.

## 5 Conclusions

The OM composition of mucilage was compared with that of PGA, and the spatial variability within a mucilage droplet was analyzed at two different scales using FTIR and micro-FTIR spectroscopy. The differences in the OM composition between PGA and mucilage suggest that the use of PGA to simulate the behavior of mucilage is questionable with respect to potential wettability and sorption properties. The FTIR spectra from central and rim regions of a freeze-dried mucilage droplet and micro-FTIR spectra from transect points revealed a spatially variable OM composition at both, the milli- and the micrometer scales. The reasons for spatial variability of mucilage OM composition could only be speculated and may depend on local exudation conditions. The shifts in O–H and C=O band maxima in FTIR of mucilage as compared to PGA seem to indicate an increase in the intra-molecular hydrogen bondings that can be caused by local differences in water or cation contents. The observed composition of mucilage OM may help explaining effects of mucilage on preferential transport processes along decayed root channels in structured soils.

## Acknowledgments

This study was financially supported by the German Federal Ministry of Food and Agriculture (BMEL) and the Ministry for Science, Research and Culture of the State of Brandenburg (MWFK). We thank Andrea Carminati (University of Bayreuth) for his suggestions and comments to the manuscript.

## References

- Ahmed, M. A., Kroener, E., Holz, M., Zarebanadkouki, M., Carminati, A. (2014): Mucilage exudation facilitates root water uptake in dry soils. *Funct. Plant Biol.* 41, 1129–1137.
- Ahmed, M. A., Holz, M., Woche, S. K., Bachmann, J., Carminati, A. (2015): Effect of soil drying on mucilage exudation and its water repellency: a new method to collect mucilage. *J. Plant Nutr. Soil Sci.* 178, 821–824.
- Ahmed, M. A., Banfield, C. C., Sanaullah, M., Gunina, A., Dippold, M. A. (2018a): Utilisation of mucilage C by microbial communities under drought. *Biol. Fertil. Soils* 54, 83–94.
- Ahmed, M. A., Sanaullah, M., Blagodatskaya, E., Mason-Jones, K., Jawad, H., Kuzyakov, Y., Dippold, M. A. (2018b): Soil microorganisms exhibit enzymatic and priming response to root mucilage under drought. *Soil Biol. Biochem.* 116, 410–418.
- Angst, G., Kögel-Knabner, I., Kirfel, K., Hertel, D., Mueller, C. W. (2016): Spatial distribution and chemical composition of soil organic matter fractions in rhizosphere and non-rhizosphere soil under European beech (*Fagus sylvatica* L.). *Geoderma* 264, 179–187.
- Bassan, P., Byrne, H. J., Lee, J., Bonnier, F., Clarke, C., Dumas, P., Gazi, E., Brown, M. D., Clarke, N. W., Gardner, P. (2009): Reflection contributions to the dispersion artefact in FTIR spectra of single biological cells. *Analyst* 134, 1171–1175.
- Capriel, P. (1997): Hydrophobicity of organic matter in arable soils: influence of management. *Eur. J. Soil Sci.* 48, 457–462.
- Carminati, A., Vetterlein, D. (2013): Plasticity of rhizosphere hydraulic properties as a key for efficient utilization of scarce resources. *Ann. Bot.* 112, 277–290.
- Carminati, A., Benard, P., Ahmed, M. A., Zarebanadkouki, M. (2017): Liquid bridges at the root–soil interface. *Plant Soil* 417, 1–15.
- Carvalho, L. C., Dennis, P. G., Fedoseyenko, D., Hajirezaei, M. R., Borriss, R., von Wirén, N. (2011): Root exudation of sugars, amino acids, and organic acids by maize as affected by nitrogen, phosphorus, potassium, and iron deficiency. *J. Plant Nutr. Soil Sci.* 174, 3–11.
- Celi, I., Schnitzer, M., Negre, M. (1997): Analysis of carboxylic groups in soil humic acids by a wet chemical method, FT-IR spectrometry and solution  $^{13}\text{C}$  NMR: A comparative study. *Soil Sci.* 162, 189–197.
- Chen, F. X., Arye, G. (2017): The role of lipids and polysaccharides in model root mucilage with implications for the surface activity of the rhizosphere. *Biologia* 72, 1285–1290.
- Cheng, Y., Ogden, F. L., Zhu, J. (2017): Earthworms and tree roots: A model study of the effect of preferential flow paths on runoff generation and groundwater recharge in steep, saprolitic, tropical lowland catchments. *Water Resour. Res.* 53, 5400–5419.
- Chenu, C., Le Bissonnais, Y., Arrouays, D. (2000): Organic matter influence on clay wettability and soil aggregate stability. *Soil Sci. Soc. Am. J.* 64, 1479–1486.
- Clapp, C. E., Hayes, M. H. B., Swift, R. S. (1993): Isolation, Fractionation, Functionalities, and Concepts of Structures or Soil Organic Macromolecules, in Beck, A. J., Jones, K. C., Hayes, M. H. B., and Mingelgrin, U. (eds.): Organic Substances in Soil and Water: Natural Constituents and Their Influences on Contaminant Behaviour. The Royal Society of Chemistry. Cambridge, UK, pp. 31–68.
- Czarnes, S., Hallett, P. D., Bengough, A. G., Young, I. M. (2000): Root- and microbial-derived mucilages affect soil structure and water transport. *Eur. J. Soil Sci.* 51, 435–443.
- Demyan, M. S., Rasche, F., Schulz, E., Breulmann, M., Müller, T., Cadisch, G. (2012): Use of specific peaks obtained by diffuse reflectance Fourier transform mid-infrared spectroscopy to study the composition of organic matter in a Haplic Chernozem. *Eur. J. Soil Sci.* 63, 189–199.
- Di Marsico, A., Scrano, L., Labella, R., Lanzotti, V., Rossi, R., Cox, L., Perniola, M., Amato, M. (2018): Mucilage from fruits/seeds of chia (*Salvia hispanica* L.) improves soil aggregate stability. *Plant Soil* 425, 57–69.
- Ellerbrock, R. H., Höhn, A., Gerke, H. H. (1999): Characterization of soil organic matter from a sandy soil in relation to management practice using FT-IR spectroscopy. *Plant Soil* 213, 55–61.
- Ellerbrock, R. H., Gerke, H. H. (2004): Characterizing organic matter of soil aggregate coatings and biopores by Fourier transform infrared spectroscopy. *Eur. J. Soil Sci.* 55, 219–228.
- Ellerbrock, R. H., Gerke, H. H., Bachmann, J., Goebel, M.-O. (2005): Composition of organic matter fractions for explaining wettability of three forest soils. *Soil Sci. Soc. Am. J.* 69, 57–66.
- Ellerbrock, R. H., Gerke, H. H., Böhm, C. (2009): In situ DRIFT characterization of organic matter composition on soil structural surfaces. *Soil Sci. Soc. Am. J.* 73, 531–540.
- Ellerbrock, R. H., Gerke, H. H. (2013): Characterization of organic matter composition of soil and flow path surfaces based on physicochemical principles—A review. *Adv. Agron.* 121, 117–177.
- Gaume, A., Weidler, P. G., Frossard, E. (2000): Effect of maize root mucilage on phosphate adsorption and exchangeability on a synthetic ferrihydrite. *Biol. Fertil. of Soils* 31, 525–532.
- Gerke, H. H. (2006): Preferential flow descriptions for structured soils. *J. Plant Nutr. Soil Sci.* 169, 382–400.
- Gerzabek, M. H., Antil, R. S., Kögel-Knabner, I., Knicker, H., Kirchmann, H., Haberhauer, G. (2006): How are soil use and management reflected by soil organic matter characteristics: A spectroscopic approach. *Eur. J. Soil Sci.* 57, 485–494.
- Gessa, C., Deiana, S. (1992): Ca-polygalacturonate as a model for a soil-root interface. *Plant Soil* 140, 1–13.
- Gottwald, W., Wachter, G. (1997): IR-Spektroskopie für Anwender. Wiley-VCH. Weinheim, Germany.
- Gregory, P. J., Bengough, A. G., George, T. S., Hallett, P. D. (2013): Rhizosphere engineering by plants: Quantifying soil–root interactions. *Adv. Agric. Syst. Model. Transdis. Res. Synth. Appl.* 4, 1–30.
- Haas, C., Gerke, H. H., Ellerbrock, R. H., Hallett, P. D., Horn, R. (2018): Relating soil organic matter composition to soil water repellency for soil biopore surfaces different in history from two Bt horizons of a Haplic Luvisol. *Ecohydrology* 11. DOI: <https://doi.org/10.1002/eco.1949>.
- Haberhauer, G., Gerzabek, M. H. (1999): DRIFT and transmission FT-IR spectroscopy of forest soils: An approach to determine decomposition processes of forest litter. *Vibr. Spectrosc.* 19, 413–417.
- Holz, M., Leue, M., Ahmed, M. A., Benard, P., Gerke, H. H., Carminati, A. (2018): Spatial distribution of mucilage in the rhizosphere measured with infrared spectroscopy. *Front. Environ. Sci.* 6. DOI: <https://doi.org/10.3389/fenvs.2018.00087>.

- Jarvis, N. J. (2007): A review of non-equilibrium water flow and solute transport in soil macropores: principles, controlling factors and consequences for water quality. *Eur. J. Soil Sci.* 58, 523–546.
- Jones, D. L., Edwards, A. C. (1998): Influence of sorption on the biological utilization of two simple carbon substrates. *Soil Biol. Biochem.* 30, 1895–1902.
- Jones, D. L., Nguyen, C., Finlay, R. D. (2009): Carbon flow in the rhizosphere: carbon trading at the soil–root interface. *Plant Soil* 321, 5–33.
- Kaiser, R., Gottschalk, G. (1972): Elementare Tests zur Beurteilung von Meßdaten. Hochschultaschenbücher Band 774, Bibliographisches Inst., Mannheim, Germany.
- Kaiser, M., Ellerbrock, R. H., Gerke, H. H. (2008): Cation exchange capacity and composition of soluble soil organic matter fractions. *Soil Sci. Soc. Am. J.* 72, 1278–1285.
- Kögel-Knabner, I. (1997):  $^{13}\text{C}$  and  $^{15}\text{N}$  NMR spectroscopy as a tool in soil organic matter studies. *Geoderma* 80, 243–270.
- Kögel-Knabner, I. (2017): The macromolecular organic composition of plant and microbial residues as inputs to soil organic matter: Fourteen years on. *Soil Biol. Biochem.* 105, A3–A8.
- Kroener, E., Zarebanadkouki, M., Kaestner, A., Carminati, A. (2014): Nonequilibrium water dynamics in the rhizosphere: How mucilage affects water flow in soils. *Water Resour. Res.* 50, 6479–6495.
- Leue, M., Gerke, H. H., Ellerbrock, R. H. (2013): Millimetre-scale distribution of organic matter composition at intact biopore and crack surfaces. *Eur. J. Soil Sci.* 64 (6), 757–769.
- Leue, M., Wohld, A., Gerke, H. H. (2018): Two-dimensional distribution of soil organic carbon at intact macropore surfaces in BT-horizons. *Soil Till. Res.* 176, 1–9.
- Lin, K.-Y., Daniel, J. R., Whistler, R. L. (1994): Structure of chia seeds polysaccharide exudate. *Carbohydr. Polym.* 23, 13–18.
- Marx, M., Buegger, F., Gatteringer, A., Zsolnay, Á., Munch, J. C. (2007): Determination of the fate of  $^{13}\text{C}$  labelled maize and wheat exudates in an agricultural soil during a short-term incubation. *Eur. J. Soil Sci.* 58, 1175–1185.
- McCully, M. E. (1999): Roots in soil: Unearthing the complexities of roots and their rhizospheres. *Annu. Rev. Plant Physiol. Plant Mol. Biol.* 50, 695–718.
- Mikutta, C., Lang, F., Kaupenjohann, M. (2006): Kinetics of phosphate sorption to polygalacturonate-coated goethite. *Soil Sci. Soc. Am. J.* 70, 541–549.
- Mimmo, T., Marzadori, C., Francioso, O., Deiana, S., Gessa, C. E. (2003): Effects of aluminum sorption on calcium-polygalacturonate network used as soil–root interface model. *Biopolymers* 70, 655–661.
- Morel, J. L., Andreux, F., Habbib, L., Guckert, A. (1987): Comparison of the adsorption of maize root mucilage and polygalacturonic acid on montmorillonite homoionic to divalent lead and cadmium. *Biol. Fertil. Soils* 5, 13–17.
- Muñoz, L. A., Cobos, A., Diaz, O., Aguilera, J. M. (2012): Chia seeds: Microstructure, mucilage 523 extraction and hydration. *J. Food Engin.* 108, 216–224.
- Naveed, M., Ahmed, M. A., Benard, P., Brown, L. K., George, T. S., Bengough, A. G., Roose, T., Koebernick, N., Hallett, P. D. (2019): Surface tension, rheology and hydrophobicity of rhizodeposits and seed mucilage influence soil water retention and hysteresis. *Plant Soil* 437, 65–81.
- Nguyen, C., Froux, F., Recous, S., Morvan, T., Robin, C. (2008): Net N immobilisation during the biodegradation of mucilage in soil as affected by repeated mineral and organic fertilisation. *Nutr. Cycl. Agroecosys.* 80, 39–47.
- Ruiz, S., Or, D., Schymanski, S. J. (2015): Soil penetration by earthworms and plant roots—mechanical energetics of bioturbation of compacted soils. *PLoS ONE* 10. DOI: <https://doi.org/10.1371/journal.pone.0128914>.
- White, K. E., Reeves III, J. B., Coale, F. J. (2016): Cell wall compositional changes during incubation of plant roots measured by mid-infrared diffuse reflectance spectroscopy and fiber analysis. *Geoderma* 264, 205–213.
- Zickenrott, I. M., Woche, S. K., Bachmann, J., Ahmed, M. A., Vetterlein, D. (2016): An efficient method for the collection of root mucilage from different plant species—A case study on the effect of mucilage on soil water repellency. *J. Plant Nutr. Soil Sci.* 179, 294–302.